

CONSTRAINING THE PETROGENESIS OF THE PAIRED ACHONDRITES GRA 06128/9 THROUGH PARTIAL MELTING OF AN OXIDIZED CHONDRITE. E. S. Sosa^{1,2}, N. G. Lunning¹, T. J. McCoy¹, E. S. Bullock^{1,3}, C. M. Corrigan¹, and K. G. Gardner-Vandy⁴. ¹Department of Mineral Sciences, National Museum of Natural History, Smithsonian Institution, Washington, DC. ²Department of Geology and Environmental Geosciences, Lafayette College, Easton, PA. ³Geophysical Laboratory, Carnegie Institution of Science, Washington, DC. ⁴Department of Geosciences, The University of Tulsa, Tulsa, OK. so-sae@lafayette.edu

Introduction: With the exception of the 4.56 Ga paired achondrites Graves Nunataks 06128 and 06129 (GRA 06128/9), all asteroidal differentiated meteorites found to date have mafic or ultramafic whole rock compositions. The discovery of the feldspar-rich GRA 06128/9 meteorites, collected during the 2006-2007 U.S. Antarctic Search for Meteorites (ANSMET) season, suggests that hitherto unrecognized processes of magmatic generation operated on asteroids or small planetesimals 4.56 Ga [1].

GRA 06128/9 modal analyses indicate a bulk composition that plots in the trachyandesite to andesite fields of the total alkalis and silica (TAS) igneous rock classification diagram, with concentrations of SiO₂ and total alkalis ranging from 52.2 to 57.8 wt. % and 5.6 to 7.1 wt. %, respectively [2]. GRA 06128/9 also have relatively high concentrations of highly siderophile elements (HSEs), which usually concentrate in iron cores of rocky differentiated bodies. High concentrations of SiO₂, alkalis, and HSEs could suggest that GRA 06128/9 originated on an undifferentiated planetesimal as a primitive melt generated by low degree partial melting of a chondritic precursor. Bulk GRA 06128/9 $\Delta^{17}\text{O}$ ranges from -0.23 to -0.18 ‰, suggesting a possible shared history with the brachinite meteorite group, for which $\Delta^{17}\text{O}$ ranges from -0.31 to -0.11 ‰ [2].

Gardner-Vandy et al. [3] explored the possibility that the brachinites could represent a residue from partial melting of an R-chondrite-like precursor through 96-hour partial melting experiments of the R4 chondrite LAP 03639. These experiments found that 25% partial melting of R chondrite at IW-1 and 1250°C produced a residue equivalent to the brachinites and a melt with high concentrations of SiO₂, like GRA 06128/9. These experiments were not designed to study alkali compositions, and Na was lost during the experiments to volatilization due to experimental duration. Usui et al. [4] experimentally examined the formation of GRA 06128/9 with a different approach by partial melting H chondrite composition synthetic mixtures. However, the melts of GRA06128/9-like compositions generated in the work of [4] were at $f\text{O}_2$ conditions below those calculated by [5] for GRA06128/9. Here, we explore the formation a GRA 06128/9 composition melt through low-degree partial melting experiments of oxidized chondrite precursor using the R4 chondrite LAP 03639.

Methods: Four experiments were run at a constant $f\text{O}_2$ of IW at temperatures of 1080°C, 1100°C, 1120°C, and 1140°C. One experiment was run at 1100°C and IW+1. In each experiment, a 142.2-155.8 mg chip of the R4 chondrite LAP 03639 was heated inside an alumina crucible in a Deltech vertical tube furnace to the target temperature. $f\text{O}_2$ was controlled with a CO/CO₂ mixture to replicate the hypothesized crystallization environment of GRA 06128/9 (IW+0.5 to IW+1.5; [5]). Short-duration experiments were used to minimize the effects of Na volatilization under high temperatures around an $f\text{O}_2$ of IW. After four hours, experiments were drop-quenched in nanopure water.

Melting of an R chondrite bulk composition was modeled with MELTS software [6]. The conditions for our MELTS modeling were a bulk composition of the Rumuruti chondrite [7], $f\text{O}_2$ of IW, pressure of 0.1 MPa (~1 bar/~1 atm), and a range of temperatures (1060-1260°C), which span our experimental melting temperatures.

Semi-quantitative compositional data of the experimental glasses were obtained with a FEI Nova Nano SEM 600 field emission gun scanning electron microscope (FEG-SEM) at the Smithsonian Institution (SI). This semi-quantitative data guided field emission gun-electron microprobe analysis (FEG-EPMA) of the melts with a JEOL 8530F at the Carnegie Institution of Science, Geophysical Laboratory. Beam conditions were 10 kV, 10 nA, and 2-5 μm spot size. 102 analyses with appropriate totals (98-102%) and with no beam overlap were collected. Plagioclase, olivine, and pyroxene grains near melt pockets were measured with JEOL 8900R EMP at SI at 15 kV and 20 or 30 nA beam conditions with a 1 μm spot size.

Phase abundances were also modeled for the 1120°C and 1140°C experimental products using backwards linear regression modeling. In this modeling, the Rumuruti bulk composition of [7] was used as the whole rock composition. The experimental melt compositions from this work and silicate mineral compositions of unmelted LAP 03639 from [3] were used as the phase compositions.

Results and Discussion: The melts generated during our experiments fall within the basaltic trachyandesite to andesite fields of the TAS diagram (Fig 1), similar to the bulk compositions of GRA 06128/9 calculated

from modal analyses by [2]. The melts generated in the 1120°C and 1140°C experiments provide the closest match to the bulk composition of GRA 06128/9. The compositional differences between the IW and IW+1 1100°C experiments were statistically insignificant, suggesting that our conclusions hold true for the oxygen fugacity range of GRA 06128/9.

SiO₂ and Al₂O₃ (wt.%) in the melt decreased between our 1080°C to 1140°C experiments (i.e. decreased with higher degrees of partial melting) from ~58 to 52% and ~20 to 16%, respectively. Na₂O + K₂O, CaO, and FeO (wt.%) in the melt increased between the 1080°C and 1140°C experiments, increasing from ~4.6 to 5.5%, ~2.6 to 2.8%, and ~9.8 to 15.1%, respectively. The compositional trend from MELTS modeling does not align with the trend from our experiments. From 1080°C to 1140°C, MELTS modeling shows alkalis wt.% (Na₂O + K₂O) decreasing from ~10.2 to 5.5% and wt.% Al₂O₃ increasing from ~10.4 to 12.0% (Fig 1). Although both MELTS modeling and our experimental results show SiO₂ decreasing and FeO and CaO increasing at higher degrees of partial melting, they do not agree with respect to oxide wt.% in the melt for the 1080°C, 1100°C and 1120°C experiments: MELTS yielded under-estimates for wt.% FeO and over-estimates for wt. % SiO₂ and CaO for these experiments. Equilibrium-based MELTS modeling does, however, converge with our non-equilibrium experimental results for wt.% SiO₂, FeO, MgO, CaO, and alkalis at IW and 1140°C.

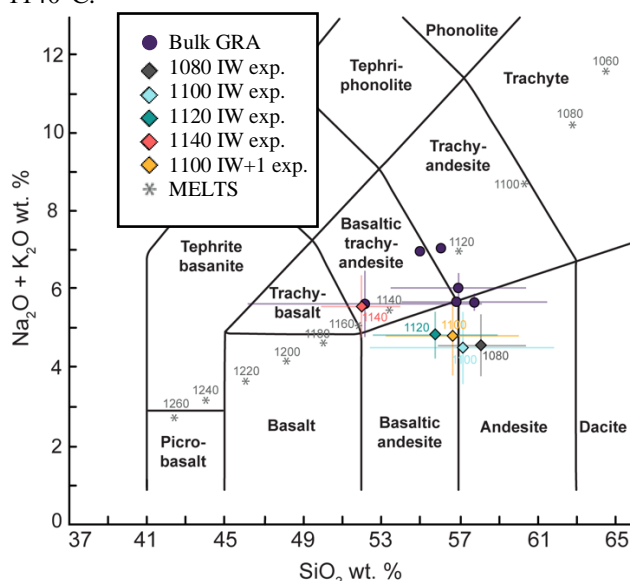


Figure 1: Total alkalis versus silica (TAS) diagram with experimental melt and MELTS modeling compositions. The range of bulk GRA 06128/9 compositions calculated by modal recombination by Day et al. (2012) is also shown. Plot modified from [8].

Backwards linear regression modeling (which modeled non-equilibrium melting because we used the composition of our experimental melt as a variable) suggests 13.6±2.0% and 22.0±2.8% partial melting occurred at 1120°C and 1140°C, respectively. MELTS modeling of equilibrium melting suggests 10.2% and 15.7% partial melting during the 1120°C and 1140°C experiments, respectively. These percent-melt results and the compositional convergence between experimental results and MELTS modeling at 1140°C suggests that regardless of whether or not equilibrium was achieved during melting the GRA 06128/9 parent melt could have been generated by ~16-20% partial melting of an R-chondrite-like precursor.

Melts generated in our experiments at higher temperatures and degrees of partial melting had higher concentrations of alkalis and lower concentration of SiO₂. At higher temperatures and higher degrees of partial melting, relatively SiO₂-poor and FeO, CaO, and MgO-rich phases like clinopyroxene and olivine likely began to melt in greater proportions as temperature increased. This resulted in the SiO₂ decrease observed for melts generated in our 1120°C and 1140°C experiments. The discrepancy in alkali concentrations between our experimental results and MELTS modeling is likely a function of non-equilibrium processes like incongruent melting and textural features of our chondritic precursor. Textural controls would likely have been especially strong in the lowest-degree melting experiments, where melting along mineral interfaces is expected to be the dominant process contributing to melt composition.

Conclusion: Our findings suggest that the parent melt for GRA 06128/9 could have been generated by a single-stage partial melting event of an oxidized chondritic precursor, similar to LAP 03639 in major element composition. Melts generated at 1140°C at the IW redox buffer provide the closest match to the whole rock major element composition of GRA 06128/9; this is supported by equilibrium MELTS modeling, non-equilibrium backwards linear regression modeling, and our non-equilibrium experimental results.

References: [1] Day J. M. D. et al. (2009) *Nature* 457, 179-182. [2] Day J. M. D. et al. (2012) *Geochem. Cosmo Acta* 81, 94-128. [3] Gardner-Vandy K. G. et al. (2013) *Geochem. Cosmo Acta* 122, 36-57. [4] Usui T. et al. (2015) *Met. Planet. Sci.* 50, 759-781 [5] Shearer C. K. et al. (2010) *Geochem. Cosmo Acta* 74, 1172-1199. [6] Asimow P. D. and Ghiorso M. S. (1998) *Am. Min.* 83, 1127-1132. [7] Jarosewich E. (2006) *Met. Planet. Sci.* 41, 1381-1382. [8] Lunning N. G. et al. (in review) *Geochem. Cosmo Acta*.